POLARIZATION OF POSITIVE MUONS IN A FREON BUBBLE CHAMBER

Thesis for the Degree of M. S.

MICHIGAN STATE UNIVERSITY

Wilbur Reed Langford

1960

POLARIZATION OF POSITIVE MUONS

IN A FREON BUBBLE CHAMBER

by

Wilbur Reed Langford

AN ABSTRACT

Submitted to the College of Science and Arts

Michigan State University of Agriculture and

Applied Science in partial fulfillment of

the requirements for the degree of

MASTER OF SCIENCE

Department of Physics

1960

Approved Joseph Ballam

ABSTRACT

The depolarization of positive mu mesons, decaying at rest, in a freon bubble chamber, has been measured by observing the decay asymmetry of the ensuing electrons. The mu mesons come from the decay of positive pions produced in a synchrocyclotron. From 1328 mu decays having electrons of energy $\gtrsim 6.9$ Mev the decay asymmetry parameter, a was found to be 0.165 ± 0.048 which corresponds to a depolarization of $50 \pm 14\%$. It thus appears that freon may be used as an analyzer for mu mesons in experiments where large numbers of these mesons are observed. An analysis of a sample of electrons with energy $\gtrsim 11.2$ Mev showed an increase of polarization with energy as predicted by Lee and Yang.

POLARIZATION OF POSITIVE MUONS
IN A FREON BUBBLE CHAMBER

by

Wilbur Reed Langford

A THESIS

Submitted to the College of Science and Arts
Michigan State University of Agriculture and
Applied Science in partial fulfillment of
the requirements for the degree of

MASTER OF SCIENCE

Department of Physics

1960

ACKNOWLEDGMENT

I am most grateful to Prof. J. Ballam for suggesting and sponsoring this research problem. His assistance during the course of the experiment, and especially with the final manuscript, is greatly appreciated. I wish to acknowledge Dr. R. Crittenden for the use of film for scanning, and also John Scandrett, James Parker, and John Boyd for their consultation. I am indeed obliged to Justin Huang for the method of determining the space angle as appears in the appendix. Special thanks go to Jerry Lamsa for his help in scanning a large portion of the film and to Jean Hill for typing the final copy of the manuscript.

TABLE OF CONTENTS

I. INTRODUCTION

In 1956, Yang and Lee[1] predicted that the muon, in the decay $\pi^+ \rightarrow \mu^+ + \nu$, should be completely polarized on the basis of non-conservation of parity and the two-component theory of the neutrino. This polarization consists of the orientation of the spin of the muon along the direction of its linear momentum. Yang and Lee also predicted that with the subsequent decay of the muon, $\mu^+ \rightarrow e^+ + \nu + \bar{\nu}$, a forward-backward asymmetry of the positive electron with respect to the direction of the muon should be observed. Confirmation of this was subsequently given by T. Coffin et al.[2] who found an asymmetry with an energy dependence consistent with the two-component prediction for the complete polarization of the muon.

However, the amount of asymmetry observed in any medium depends on the extent to which the muon is depolarized, before decay, by external fields. These fields may either be residual magnetic fields or internal atomic fields. In addition, the formation of muonium (a bound state of a positive muon with a negative electron) may also depolarize the muon. The amount of this depolarization will depend on the medium in which the decay occurs. For example, this depolarization is approximately 0% in graphite and 96% in silicon dioxide.[3]

The purpose of the present work is to measure the amount of depolarization that results in freon-13B1 ($CBrF_3$ or bromotrifluoromethane), considering the positive muon to be 100% polarized initially. Freon, which has a short radiation length, is now rather commonly used in bubble chambers whenever an investigation of processes involving gamma rays is desired.[4] These gammas usually come from π^{0} decay and bremsstrahlung of electrons. There is a class of strange particles which have alternate decays into muons or electrons. Freon chambers are used to investigate these branching ratios; for example, the following decays might be observed:

$$K^{+} \rightarrow \mu^{+} + \pi^{0} + \nu$$
$$\rightarrow e^{+} + \pi^{0} + \nu$$

$$K^{-} \rightarrow \mu^{-} + \pi^{0} + \bar{\nu}$$
$$\rightarrow e^{-} + \pi^{0} + \bar{\nu}$$

$$K^{0} \rightarrow \mu^{\pm} + \pi^{\mp} + \nu(\bar{\nu})$$
$$\rightarrow e^{\pm} + \pi^{\mp} + \nu(\bar{\nu})$$

$$\Lambda^{0} \rightarrow \mu^{-} + p + \bar{\nu}$$
$$\rightarrow e^{-} + p + \bar{\nu}$$

$$\Sigma^{+} \rightarrow \mu^{+} + n + \nu$$
$$\rightarrow e^{+} + n + \nu$$

$$\Sigma^{-} \rightarrow \mu^{-} + n + \bar{\nu}$$
$$\rightarrow e^{-} + n + \bar{\nu}$$

$$\bar{\Lambda}^{0} \rightarrow \mu^{+} + \bar{p} + \nu$$
$$\rightarrow e^{+} + \bar{p} + \nu$$

$$\bar{\Sigma}^{+} \rightarrow \mu^{+} + \bar{n} + \nu$$
$$\rightarrow e^{+} + \bar{n} + \nu$$

$$\bar{\Sigma}^{-} \rightarrow \mu^{-} + \bar{n} + \bar{\nu}$$
$$\rightarrow e^{-} + \bar{n} + \bar{\nu}$$

It might turn out to be interesting to look at the μ polarization in all of the above decay reactions and for this purpose a measurement of the amount of depolarization due to the freon itself is important.

Lee and Yang[5] found the normalized electron distribution in the decay, $\mu^+ \rightarrow e^+ + \nu + \bar{\nu}$, to be

$$dN = 2\,x^2\,[(3-2x) + (1-2x)\xi \cos\theta]\,\frac{dx\,d\Omega}{4\pi}$$

$$\text{with } x = \frac{\overline{Pe}}{\overline{Pe}\,(max)} \quad \text{and } \xi = \frac{f_V\, f_A^* + f_A\, f_V^*}{|f_V|^2 + |f_A|^2}$$

where $\overline{Pe}$ is the electron momentum and f_V and f_A represent the usual vector and axial vector coupling constants. θ, wherever it appears, is the angle between the muon and electron direction vectors. Integration of the equation for dN over all x gives

$$4\pi \frac{dN}{d\Omega} = 1 - \frac{1}{3}\xi \cos\theta.$$

For $f_r = f_A$, ξ has a maximum value of 1 so that

$$4\pi \frac{dN}{d\Omega} = 1 - \frac{1}{3} \cos\theta.$$

However, in an experiment one measures

$$4\pi \frac{dN}{d\Omega} = 1 - a \cos\theta$$

where $a = 0.33P$ and P is the polarization of the muons. Since experimental numbers for the decay of muons in carbon and hydrogen give $a = 0.26 \pm 0.02$[3], it can be assumed that the muons are approximately 100% polarized in $\pi - \mu$ decay. Thus, measurement of a in this experiment gives the depolarization of the muons by freon. The results on 1328 decays give $a = 0.165 \pm 0.048$ and therefore $P = 0.495 \pm 0.144$

which indicates that the muons are 50% depolarized by freon. For the 264 events of higher energy with the asymmetry $a = 0.313 \pm 0.107$. The depolarization is only 6%. This value shows the predicted increase of the asymmetry with muon energy. However, the depolarization due to the freon is the same, within one standard deviation, for both energy groups.

II. DESCRIPTION OF THE EXPERIMENT

A. Film Exposures

Photographs of the meson decay events were obtained from exposures made in August 1958 and February 1959 at the Carnegie Institute of Technology synchrocylotron.[6] Pi mesons were produced from the internal proton beam of the accelerator and then passed through the field of a bending and analyzing magnet. The emerging beam was moderated by a copper absorber of sufficient thickness so that pions would stop near the center of the bubble chamber. Stereo pictures were taken for each chamber expansion with the camera lenses at an angular deviation of 8 1/3° from an axis extending from the bubble chamber to a central point between the lenses. In figure I, the general physical arrangement at the cyclotron site is shown.

B. Measurement of Events

Six sets of data were taken with the following number of events in each set:

Tape	Events
Data 1	251
Data 2	269
Data 3	267
Data 4	266
Data 5	275
Data 6	264
Total	1592.

Figure 1. Experimental arrangement at the synchrocylotron at the Carnegie Institute of Technology.

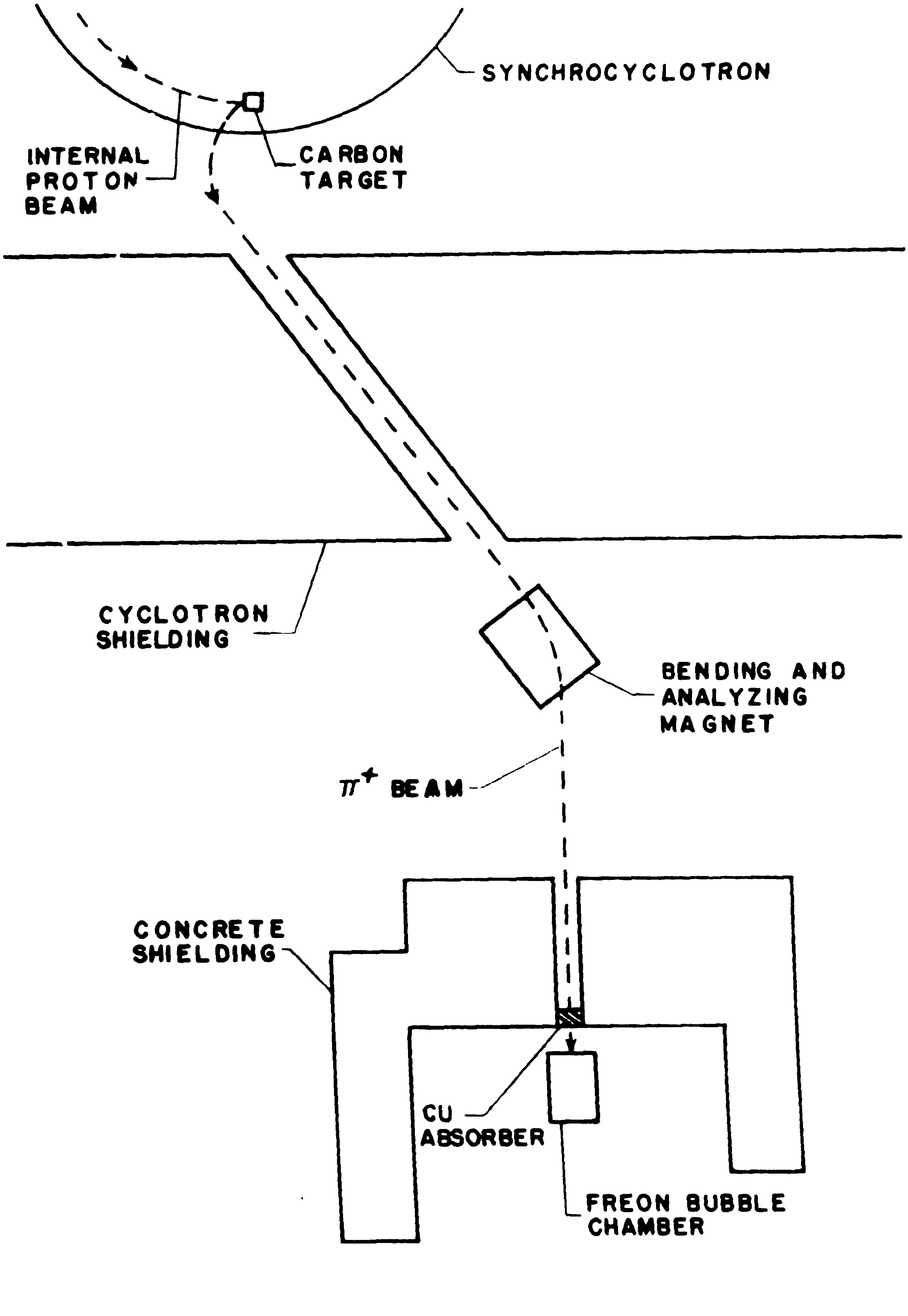
SYNCHROCYCLOTRON
INTERNAL PROTON BEAM
CARBON TARGET
CYCLOTRON SHIELDING
BENDING AND ANALYZING MAGNET
π^+ BEAM
CONCRETE SHIELDING
CU ABSORBER
FREON BUBBLE CHAMBER

Figure 1.

Scanning of the film was accomplished by projecting the stereo views (which are side by side on the film) onto a translucent screen that could be viewed from the opposite side from the projector for convenience. By means of the 10 fiducial marks (see Figure 2), uniform magnification could be achieved with the proper adjustment of the angle of the screen. The fiducial marks were also used to determine the magnification involved.

An arbitrary coordinate system was set up in the scanner plane with axes parallel to each of the sets of x and z fiducial marks on the scanning screen. The center fiducial mark on the front bubble chamber glass, designated by the subscript o, was used as the reference point. The position of this reference is used later in the computer program. All distances in the scanner plane were measured to the nearest .5mm. with the aid of two perpendicular plastic scales mounted on the arm of a drafting machine. Angles in the scanner plane were read to within .5° with the aid of a magnifier on the protractor of the drafting machine. The angles were measured with respect to the direction of the z coordinate axis of the scanner plane (which is oppositely directed to the pion beam) in a counter-clockwise direction from 0° to 360°. Angles of exactly 0° or 180° were avoided to prevent infinite values for the cotangent. The orientation of the arbitrary coordinate system was such that all parameters had positive values only. This eliminated any sign errors.

Figure 2. An example of the decays

$$\pi^+ \rightarrow \mu^+ + \nu$$
$$\mu^+ \rightarrow e^+ + \nu + \bar{\nu}$$

as was seen in the scanner plane.

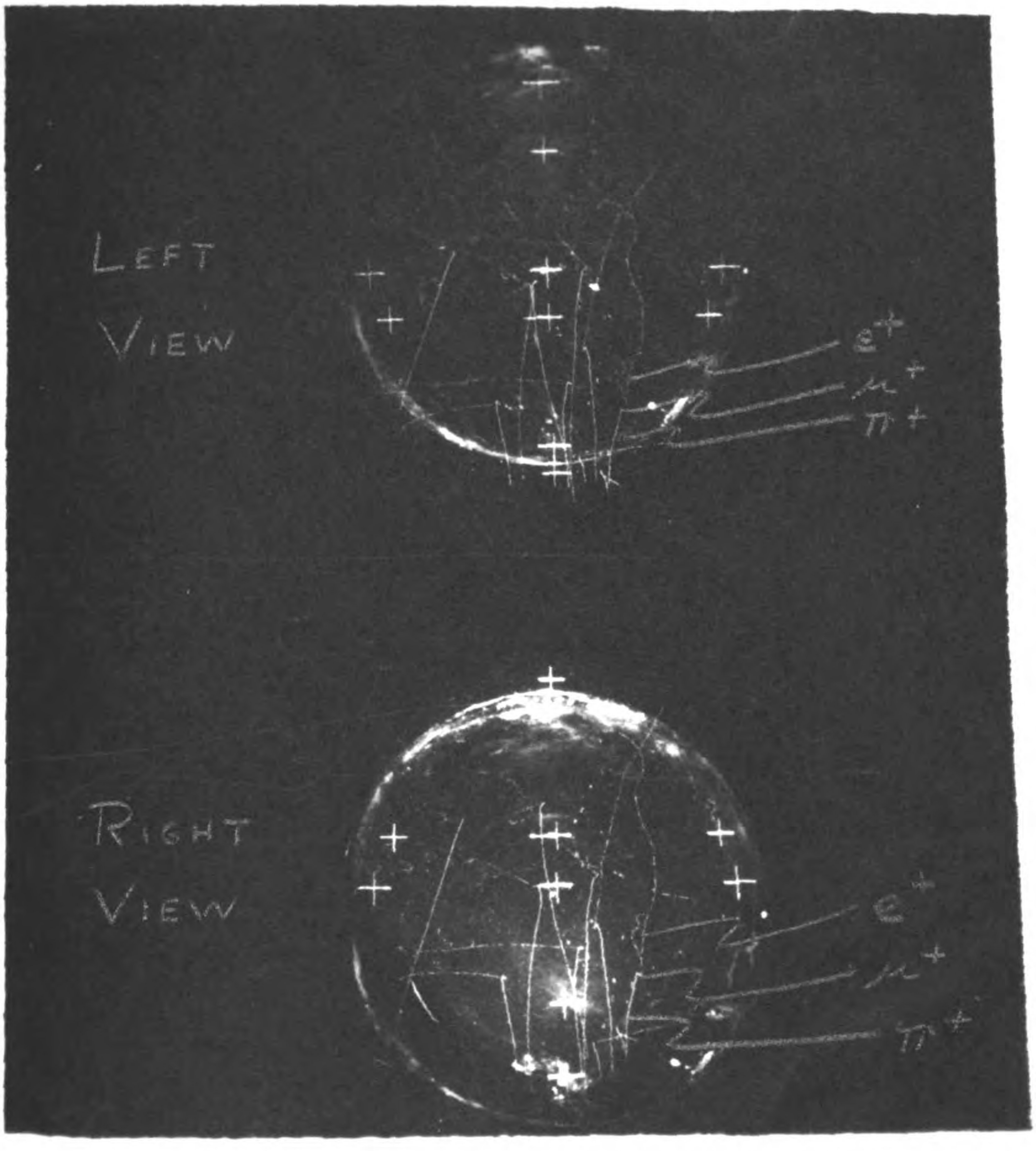

Figure 2.

Directions of muon paths of 3 mm. in length in the scanner plane (maximum length determined in computations section) are usually easily measured. However, if the path length is less than 1 mm., its direction cannot be measured accurately since this approaches the value of its width. Also, low energy positrons from mu decays have an isotropic distribution[7]; therefore, only those events were measured in which the positron path length was 5 cm. (2.78 cm. in the bubble chamber) or greater in the scanner plane. The values for the muon path length of 1 mm. to 3 mm. and the minimum value of 5 cm. for the positron path served as limits for choosing events for measurement.

With these considerations, values for the parameters

$$z_{0L},\ x_{0R},\ z_{0R},\ \theta_{2L},\ \theta_{3L}$$

$$z_{1L},\ x_{1R},\ z_{1R},\ \theta_{2R},\ \theta_{3R}$$

were measured (as required for space angle calculations in appendix I) where z_{0L} represents the coordinate of the left fiducial mark, x_{0R} and z_{0R} are the coordinates of the right fiducial mark, z_{1L}, x_{1R}, and z_{1R} are the coordinates of the muon decay point, θ_{2L} and θ_{2R} are the angles for the muon direction in the left and right views, and θ_{3L} and θ_{3R} are the corresponding angles for the positron direction.

III. CALCULATIONS

A. Required Parameters

The needed parameters for computation of the space angle in appendix I are the magnification factors m and M (defined below) and the quantities from the two views

left: z_{0L}, z_{1L}, z_{2L}, z_{3L}; θ_{2L}, θ_{3L} and

right: x_{0R}, z_{0R}; x_{1R}, z_{1R}; x_{2R}, z_{2R}; x_{3R}, z_{3R}; θ_{2R}, θ_{3R}

where z_{2L}, x_{2R}, z_{2R} are the coordinates of the projected point along the muon path and z_{3L}, x_{3R}, z_{3R} are the coordinates of a projected point along the initial direction of the positron path.

The six parameters

$$z_{2L},\ z_{3L};\ x_{2R},\ x_{3R};\ z_{2R},\ z_{3R}$$

are to be evaluated in terms of the scanning data from the two stereo views. These x and z quantities can be evaluated from projections along the mu and positron directions as follows. For the first quadrant, it is seen from the diagrams below

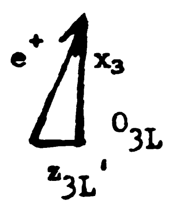

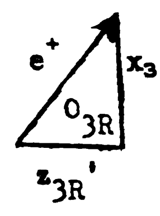

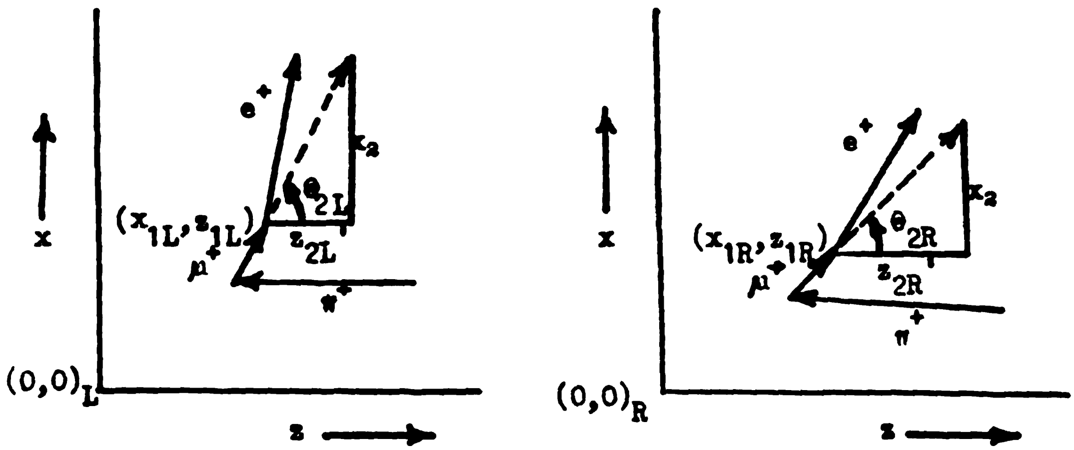

that

$$z_{2L}' = x_2 \cot \theta_{2L} \qquad \text{and} \qquad z_{2R}' = x_2 \cot \theta_{2R}$$

so that the following equations can be written directly:

$$z_{2L} = z_{1L} + z_{2L}' = z_{1L} + x_2 \cot \theta_{2L}$$

$$z_{3L} = z_{1L} + z_{3L}' = z_{1L} + x_3 \cot \theta_{3L}$$

$$x_{2L} = x_{2R} = x_{1R} + x_2$$

$$x_{3L} = x_{3R} = x_{1R} + x_3$$

$$z_{2R} = z_{1R} + Z_{2R}' = z_{1R} + x_2 \cot \theta_{2R}$$

$$z_{3R} = z_{1R} + z_{3R}' = z_{1R} + x_3 \cot \theta_{3R}.$$

$x_{2L} = x_{2R}$ and $x_{3L} = x_{3R}$ since they are equivalent vertical distances in the two views. The above six equations are valid in all four quadrants only when the following sign conventions are used:

Quadrant	x_i	z_{ij}
1	+	+
2	+	-
3	-	-
4	-	+

The magnification factors are given by the ratios

$$m = \frac{\text{unit in bubble chamber}}{\text{unit in film}}$$

$$M = \frac{\text{unit in film}}{\text{unit in scanner plane}} .$$

All of these parameters were used to find the space angle shown in appendix I. The actual space angles for the data were determined with the Mistic computer using the computer program shown in appendix II.

B. Range

Considering the rest-mass energies of 139.6 Mev and 105.7 Mev for the pi and mu mesons respectively, the kinetic energy and subsequently the range of the muon may be determined. It is easily seen from the mass defect, that the combined kinetic energy of the muon plus the neutrino is 33.9 Mev. The kinetic energy of the muon is then found to be 4.1 Mev from a two-body decay calculation. The range of a 4.1 Mev muon in freon 13B1, as projected in the scanner plane, is approximately 3 mm. as determined from range energy curves.[8]

From the rest-mass energy of a positron, considering the muon to have decayed from rest, the two body decay calculation gives the maximum kinetic energy of the emitted positron as 54.7 Mev with a corresponding range of 33.5 cm. in the scanner plane (18.6 cm. in the bubble chamber).

C. Least Squares Solution for the Asymmetry

The angular distribution of the decayed positrons for each event i may be defined by $f(x_i) = 1 + a\, x_i$ where $x_i = \cos \theta_i$.[3] The equation is normalized by integration over the solid angle, ω,

$$\int f_i \, d\omega = 2\pi \int_{-1}^{1} (1 + a\, x_i) d\, x_i = 4\pi$$

For a normalization to 1, the new equation summed over all i becomes

$$\sum_i f_i = \frac{1}{4\pi} \sum_i (1 + a\, x_i).$$

A solution for the most probable value of the asymmetry a may be derived from a method of least squares.[9] Consider the error equation

$$E^2 = \sum_i (\delta_i)^2 = \sum_i \left(f_i - \frac{1}{4\pi} - \frac{a x_i}{4\pi} \right)^2$$

where

$$\delta_i = \left(f_i - \frac{1}{4\pi} - \frac{a x_i}{4\pi}\right) \neq 0$$

is the difference equation between the observed values f_i and the theoretical values $\frac{1}{4\pi} (1 + a\, x_i)$. The error equation may be minimized for the best value of a by taking the partial derivative with respect to a, i.e.,

$$\frac{\partial E^2}{\partial a} = - \sum_i \frac{f_i x_i}{2\pi} + \sum_i \frac{x_i}{8\pi^2} + \sum_i \frac{a\, x_i^2}{8\pi^2} = 0$$

where

$$\frac{\partial f}{\partial a} = 0$$

since f_i is a measured quantity in the error equation and hence dependent only upon the data and not upon a. From the minimized equation

$$a = \frac{4\pi \sum_i f_i\, x_i - \sum_i x_i}{\sum_i x_i^2} = \frac{4\,\pi \sum_i f_i\, x_i}{\sum_i x_i^2}$$

noting that $\sum_i x_i = 0$ in the interval $-1 \leq x_i \leq 1$. The error or deviation in a is found from the following equations by using an error equation[10] for $(\delta a)^2$:

$$(\delta a)^2 = \sum_i (\frac{\partial a}{\partial Ni} \delta Ni)^2 \approx (\delta Ni)^2 \sum_i (\frac{\partial a}{\partial Ni})^2$$

but

$$a(\ldots, f_i, \ldots) = \frac{4\pi \sum_i f_i x_i - \sum_i x_i}{\sum_i x_i^2} = \frac{4\pi \sum_i f_i x_i}{\sum_i x_i^2}$$

and from an equation below $f_i = \frac{1}{2\pi} \frac{\Delta Ni}{\Delta x_i}$

hence,

$$\frac{\partial a}{\partial Ni} = \frac{\partial a}{\partial f_i} \frac{\Delta f_i}{\Delta N_i} = \frac{4\pi x_i}{\sum_i x_i^2} \cdot \frac{1}{2\pi \Delta x_i}$$

such that for $\Delta x_i = .1$

$$\delta a = \frac{20}{\sqrt{N_i} \sqrt{\sum_i x_i^2}}$$

which when normalized for 20 intervals along x_i gives

$$\delta a = \frac{1}{\sqrt{\bar{N}_i} \sqrt{\sum_i x_i^2}}$$

where $\delta N_i = \frac{\bar{N}_i}{N_i}$ and ($\bar{N}_i$ is the number of events occuring with an angular distribution on X_i or) $\bar{N}_i = \frac{1328}{20} = 66.4$ for the 1328 events or $\bar{N}i = \frac{264}{20} = 13.2$ for the set of 264 events. Though f_i is a measured quantity, the following analysis is essential for determining its value from the results of the computations. The differential number of events, dN, may be defined as $dN = f(\theta)\, 2\pi \sin\theta\, d\theta$ or

$$\sum_i f_i = \frac{1}{2\pi} \sum_i \frac{\Delta N_i}{\Delta \cos\theta_i} = \frac{1}{2\pi} \cdot \frac{\sum_i \Delta N_i}{\Delta x_i}$$

For differential values of the cosine of the space angle equal to .1 ($\Delta x_i = .1$)

$$\sum_i f_i = \frac{10}{2\pi} [\Delta N_1 + \Delta N_2 + \ldots]$$

which when normalized for N events gives

$$f_i = \frac{10}{2\pi} \cdot \frac{\Delta N_i}{N}$$

Values for f_i are obtained, in this manner, for substitution into the equation for a. The average statistical variation in N_i may be found from the square root of the mean, which when normalized gives

$$\delta N_i = \frac{\sqrt{\bar{N}_i}}{\bar{N}_i} .$$

D. Depolarization due to an External Magnetic Field

The depolarization of the muon due to its precession in a magnetic field may be determined from the following analysis. Consider the precessional frequency of an electron

$$\omega_e = \frac{\mu_e H}{2\hbar}$$

where

$$\omega_e = \frac{e H}{2m_e c} \qquad \text{and} \qquad \mu_e = \frac{e \hbar}{m_e c} .$$

Analogously, assuming the gyromagnetic ratio g of the muon to be the same as that for an electron[11], the precessional frequency of the muon is

$$\omega_\mu = \frac{\mu_e H}{2 m_\mu \hbar}$$

which gives an angular deviation in time Δt of

$$\Delta \theta = \frac{\mu_e H}{2 m_\mu \hbar} \Delta t$$

where m_μ is in terms of m_e. The above equations are only valid for a field perpendicular to the magnetic moment of the muon. From the diagram, assuming symmetry in ϕ,

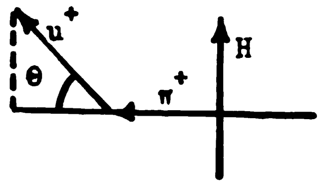

the correct equation for $\Delta\theta$ is seen to be

$$\Delta\theta = \frac{\mu_e H \cos\theta}{2 m_\mu \hbar} \Delta t .$$

The average angular deviation is given by this last equation if the average value for the cos θ is determined. An average value is found from the integral of the cosine divided by the range of the limits, i.e.,

$$\frac{\int_0^{\pi/2} \cos\theta \, d\theta}{\pi/2} = .636$$

The average angular deviation for the muon with a mean life of 2.2×10^{-6} sec. in a field of about 4 gauss (at the bubble chamber) is found to be .12 radian. This is only about a factor of two greater than the maximum error in angle measurement and is deemed negligible.

IV. RESULTS AND DISCUSSION

The results of the first five sets of data for 1328 events gave an absolute value of $|a| = 0.165 \pm 0.048$. The additional set of 264 events in data 6 was scanned for positrons with a track length equal to or greater than 8 cm. in the scanner plane (4.44 cm. in the freon bubble chamber.) This last set of data showed a larger value of $|a| = 0.313 \pm 0.107$ for the higher energy particles.

The equation for the normalized electron distribution was integrated to correspond to the energy range of the measured positrons. With the electron energy E_e and

$$x \approx \frac{E_e}{E_e\,(\text{max.})}$$

the equation for the positron track of length, $L \geq 2.78$ cm., and energy, $E \geq 6.9$ Mev[8], became

$$4\pi \frac{dN}{d\Omega} = .996 - .334\,\xi \cos\theta$$

and for the positron with track length, $L \geq 4.44$ cm., and energy, $E \geq 11.2$ Mev, it bacame

$$4\pi \frac{dN}{d\Omega} = .986 - .337\,\xi \cos\theta$$

where the maximum energy was considered to be 55.2 Mev. This variance from the equation

$$4\pi \frac{dN}{d\Omega} = 1 - \frac{1}{3}\,\xi \cos\theta$$

Figure 3. The spacial distribution of $N' = \frac{dN}{N\ d(\cos\theta)} \times 10^{-4}$ for 1328 events plotted against $\cos\theta$ where $E_e \geq 6.9$ Mev.

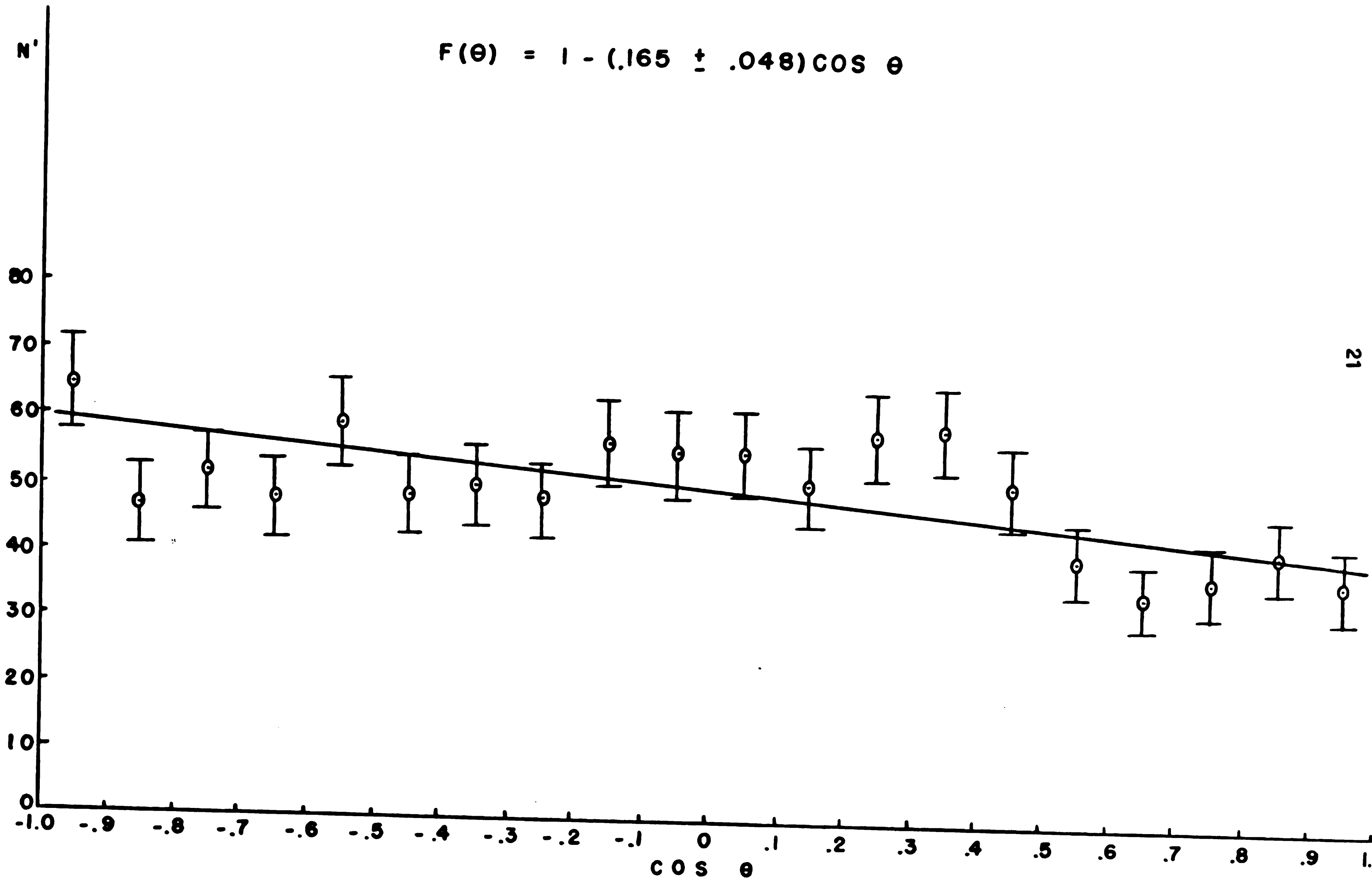

N'
F(Θ) = 1 - (.165 ± .048) COS Θ
80
70
60
50
40
30
20
10
0
-1.0
-.9
-.8
-.7
-.6
-.5
-.4
-.3
-.2
-.1
0
.1
.2
.3
.4
.5
.6
.7
.8
.9
1.0
COS Θ

Figure 3.

Figure 4. The spacial distribution of $N' = \frac{dN}{N\, d(\cos \theta)} \times 10^{-4}$ for 264 events plotted against cos θ where $E_e \geq 11.2$ Mev.

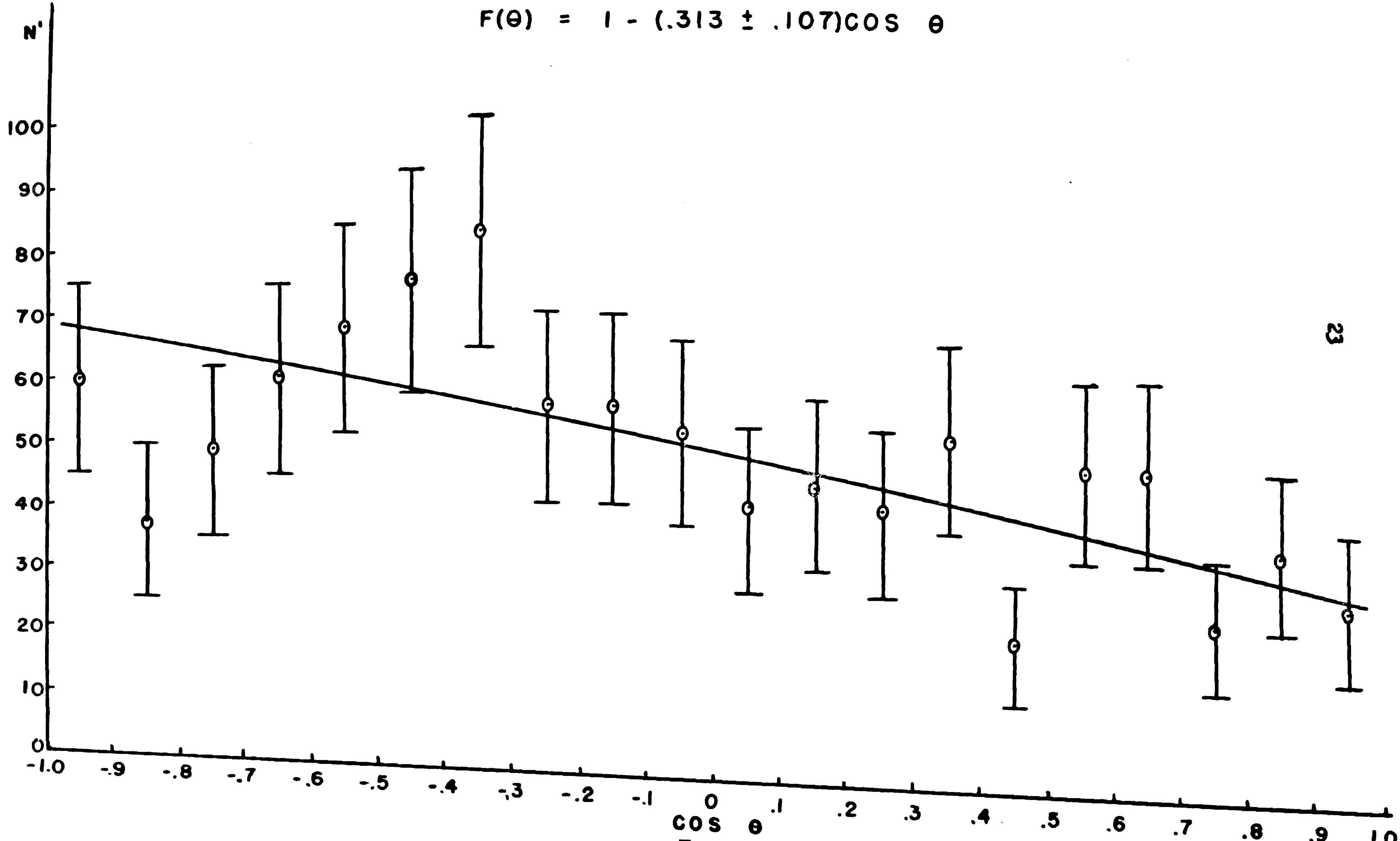
F(θ) = 1 - (.313 ± .107)COS θ
N'
100
90
80
70
60
50
40
30
20
10
0
-1.0
-.9
-.8
-.7
-.6
-.5
-.4
-.3
-.2
-.1
0
.1
.2
.3
.4
.5
.6
.7
.8
.9
1.0
COS θ

Figure 4.

is insignificant with respect to the error of this experiment. However, the increase in a with increased electron momentum is in accord with the predictions of Lee and Yang.[5] This increase in the asymmetry with increased electron momentum, for the energies used here, is also seen from the equation

$$4\pi \frac{dN}{d\Omega} = 1 - a \cos \theta$$

when it is noted that ΔN_i increases with increased electron momentum as shown in the electron spectrum for μ^+ decay.[12]

The errors in a, occuring from the measurements, are of a purely statistical nature. Any systematic change, due to the external magnetic field, has been neglected as being small.

As a result of the foregoing measurements, it seems that the depolarization effects in freon are approximately the same as in nuclear emulsions.[3] This means that a considerable number of events involving muon decays must be measured before a 10% measurement on the asymmetry can be achieved. However, with the advent of large chambers and intense beams of strange particles, freon is not an impractical medium for observing these particles.

Unfortunately very little can be said regarding the detailed mechanism by which the muons are depolarized. Present evidence shows a large range of polarizations which depend on purity of material as well as the material itself.[3]

APPENDIX I[13]

DETERMINATION OF THE SPACE ANGLE

A. Coordinate Transformations

1. Measurements made with respect to the scanning coordinate axes may be transformed to a coordinate system with respect to the front fiducial mark by the equations,

$$z_{iL}' = z_{OL} - z_{iL}$$

$$x_{iR}' = x_{iR} - x_{OR}$$

$$z_{iR}' = z_{OR} - z_{iR},$$

where i = 1 indicates the mu decay point, i = 2 indicates an arbitrary point along the projected mu direction, and i = 3 indicates an arbitrary point along the electron path or the projected electron path whenever the path does not continue on a straight course from its original direction. The sign of the primed coordinates is dictated by the pion beam direction and the center fiducial mark (+) as shown below in the left and right scanning views designated by the subscripts L and R.

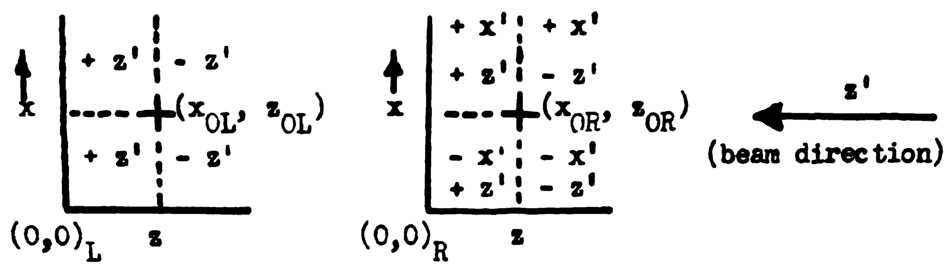

Figure 5. Diagram of space coordinate systems and planes for the calculation of the space angle (between the muon and positron direction vectors) from measurements in the two stereo projections. This diagram, however, exemplifies the coordinate systems with respect to the optical axis of the camera for the right view.

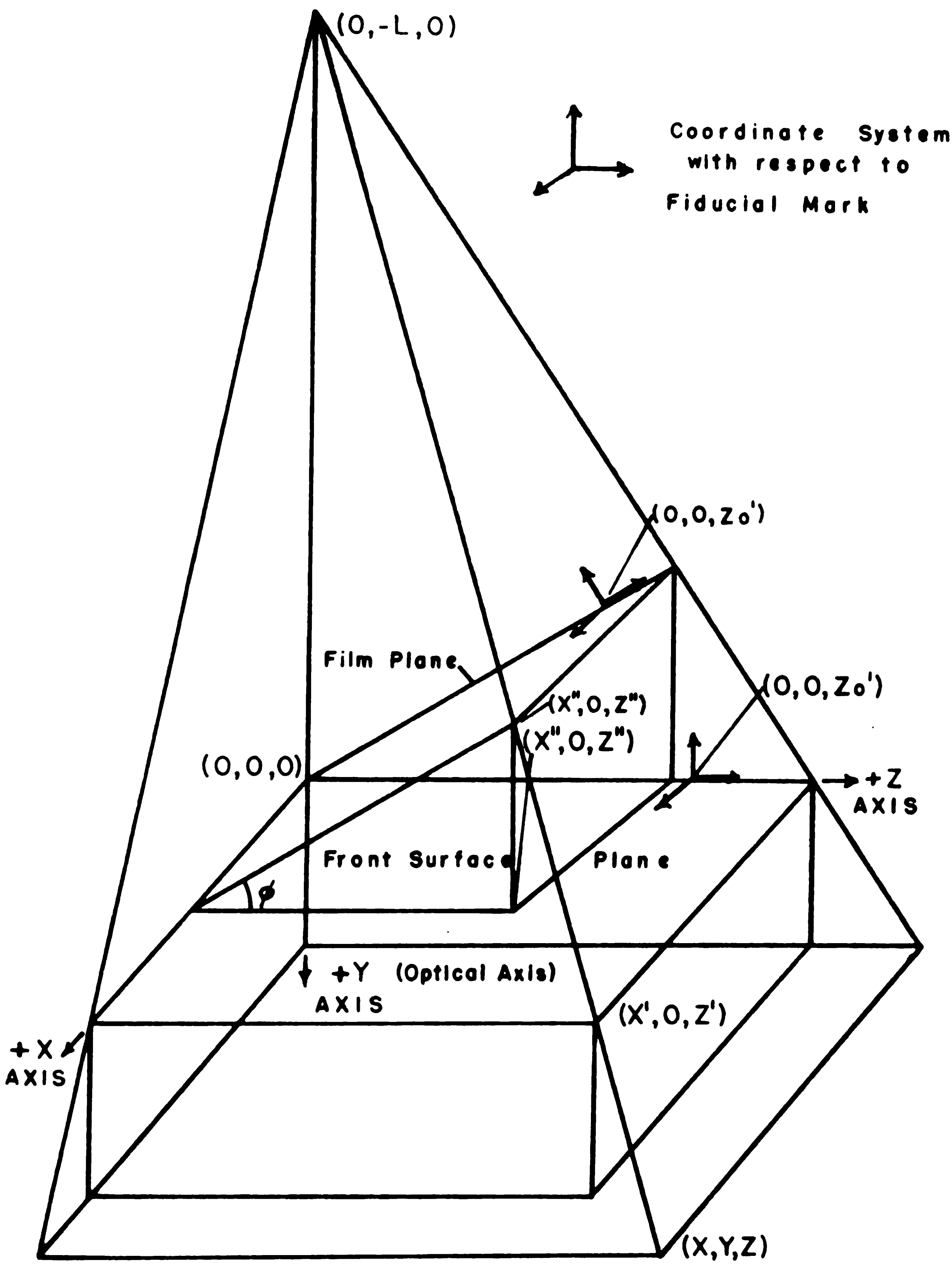
(O,-L,O)
Coordinate System with respect to Fiducial Mark
(O,O,Zo')
Film Plane
(X",O,Z")
(X",O,Z")
(O,O,Zo')
(O,O,O)
+Z AXIS
Front Surface Plane
ø
+Y (Optical Axis) AXIS
(X',O,Z')
+X AXIS
(X,Y,Z)

Figure 5.

2. Using the magnification factor M, which is equal to the ratio of a unit in the film plane to a unit in the scanner plane, the three preceeding primed parameters transfer to a coordinate system in the film plane with respect to the optical axis of the cameras as follows:

$$z_{iL}'' = z_{OL}' - Mz_{iL}'$$

$$z_{iR}'' = Mx_{iR}'$$

$$z_{iR}'' = z_{OR}' + Mz_{iR}' .$$

The signs in these equations are consistent with the sign convention illustrated in the diagram on page 25.

3. The transformation of the parameters, with respect to the optical axis, into the plane of the front surface of the bubble chamber gives the parameters Z''_{iL} , X''_{iR} , and Z''_{iR} in terms of the double primed coordinate parameters. This transformation is made with the magnification factor m, which is the ratio of a unit in the bubble chamber to a unit in the film plane, and the aid of the triangles below.

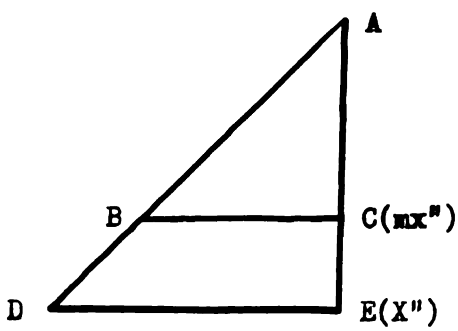

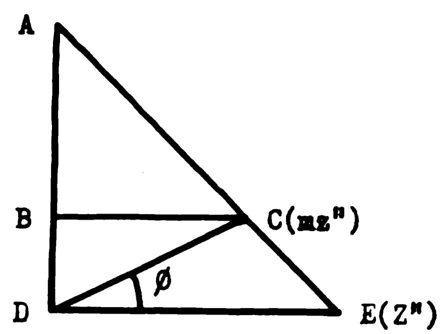

$AE = L$

$AC = L - mz''\sin\phi$

$BC = mx''$

$DE = X''$

$AB = L - mz''\sin\phi$

$AD = L$

$BC = mz''\cos\phi$

$DE = Z''$

From similar triangles ABC and ADE of the left diagram it is seen that

$$\frac{L}{L - mz''\sin \phi} = \frac{X''}{mx''}$$

or for X"

$$X'' = \frac{mx''}{(1 - mz''\sin \phi/L)} \ .$$

Likewise from the triangles ABC and ADE of the right diagram

$$Z'' = \frac{mz''\cos \phi}{(1 - mz''\sin \phi/L)} \ .$$

These last two equations may be expressed in a simpler form by using a binomial expansion. Thus, considering the left and right stereo views, the expression:

$$Z_{iL}'' = m_L z_{iL}''\cos \phi_L(1 + m_L\sin \phi_L z_{iL}''/L_L)$$

$$X_{iR}'' = m_R x_{iR}''(1 + m_R\sin \phi_R z_{iR}'')$$

$$Z_{iR}'' = m_R z_{iR}'' \cos \phi_R(1 + m_R\sin \phi_R z_{iR}''/L_R)$$

are obtained.

4. To refer X" and Z" (which are with respect to the optical axis) back to the coordinate system with respect to the front fiducial mark (Z_{OL}', Z_{OR}'), the following equations are used:

$$Z_{iL}' = Z_{OL} - Z_{iL}''$$

$$X_{iR}' = X_{iR}''$$

$$Z_{iR}' = Z_{iR}'' - Z_{OR}' \ .$$

5. The final transformation to space coordinates within the bubble chanber can be made considering the following pyramidal figure.

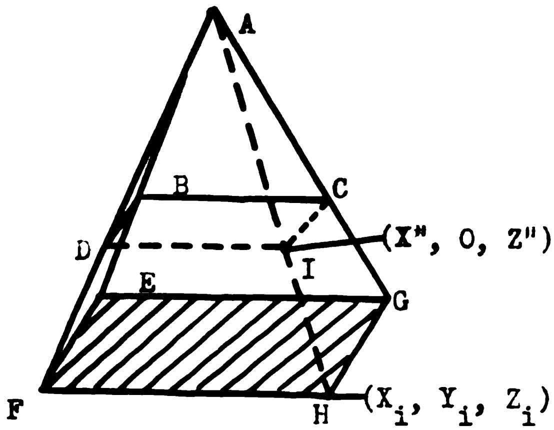

$AB = L_R$

$AE = L_R + Y_i/n$

$BC = Z_{iR}'' = Z_{OR}' + Z_{iR}'$

$EG = Z_{OR}' + Z_i$

$DB = X_{iR}'' = X_{iR}'$

$EF = X_i$

From triangles ABC and AEG,

$$\frac{L_R}{L_R + Y_i/n} = \frac{Z_{iR}''}{Z_{OR}' + Z_i} = \frac{Z_{OR}' + Z_{iR}'}{Z_{OR}' + Z_i}$$

and similarly for the corresponding left view,

$$\frac{L_L}{L_L + Y_i/n} = \frac{Z_{iL}''}{Z_{OL}' + Z_i} = \frac{Z_{OL}' + Z_{iL}'}{Z_{OL}' + Z_i}$$

it is possible to obtain the space coordinate in the Y direction,

$$Y_i = \frac{Z_{iL}' - Z_{iR}'}{\frac{Z_{iR}''}{nL_R} + \frac{Z_{iL}''}{nL_L}} ,$$

and in the Z direction,

$$Z_i = (1 + Y_i/nL_R)Z_{iR}'' - Z_{OR}' ,$$

where Z_{OR}' and Z_{OL}' are the measured distances from the camera axis to the front fiducial mark for the two views. From the triangles

ABD and AEF,

$$\frac{L_R}{L_R + Y_i/n} = \frac{X_{iR}'}{X_i}$$

so that the X coordinate is found to be,

$$X_i = (1 + Y_i/nL_R)X_{iR}' \quad .$$

The equations of section A give X_i, Y_i, and Z_i in terms of the quantities z_{OL}, x_{OR}, z_{OR}, z_{iL}, x_{iR}, and z_{iR} and the constants $m_L \sin\theta_L/L_L$, $m_L \cos\theta_L$, $m_R \sin\theta_R/L_L$, $m_R \cos\theta_R$, m_R, M, z_{OL}', z_{OR}', Z_{OL}', Z_{OR}', $1/nL_L$, and $1/nL_R$.

B. Cos of the Space Angle

The muon and electron direction vectors are defined by

$$\bar{r}_2 = \bar{r}_2(X_2 - X_1,\ Y_2 - Y_1,\ Z_2 - Z_1)$$

$$\bar{r}_3 = \bar{r}_3(X_3 - X_1,\ Y_3 - Y_1,\ Z_3 - Z_1)$$

respectively. The cosine of the space angle θ_{23} is then

$$\cos\theta_{23} = \frac{\bar{r}_2 \cdot \bar{r}_3}{|\bar{r}_2||\bar{r}_3|} = \frac{(X_2-X_1)(X_3-X_1) + (Y_2-Y_1)(Y_3-Y_1) + (Z_2-Z_1)(Z_3-Z_1)}{\sqrt{(X_2-X_1)^2 + (Y_2-Y_1)^2 + (Z_2-Z_1)^2}\sqrt{(X_3-X_1)^2 + (Y_3-Y_1)^2 + (Z_3-Z_1)^2}}$$

The space angle may easily be determined from trigonometry tables for values obtained by evaluating the equations of section A and B.

APPENDIX II

COMPUTER PROGRAM

A. Computer Tape Sequence

Tape Order Input (Library, DOI)

Preset Parameters (OO 3K)

S4 Constants

S5 Sin-Cos Subroutine (Library, T5)

S6 Square Root Subroutine (Library, R1)

S7 Cot Subroutine

S8 Print Out Subroutine (Library, P17)

S9 Temporary Storage (allocation, not on tape)

SK Data Input Subroutine (Library, N2)

SS Address Change Constants

Heading (tape print out)

Master Program

Black Switch Transfer Order (24 470N)

S3 Data (separate Tape)

White Switch Transfer Orders (OF F 26 159L)

S3 Data (additional data tapes)

B. Scaling of Parameters

1. S3 Data

0) $z_{OL} \times 10^{-4}$
1) $z_{1L} \times 10^{-4}$
2) $\theta_{2L} \times 10^{-3}$
3) $\theta_{3L} \times 10^{-3}$
4) $x_{OR} \times 10^{-4}$
5) $z_{OR} \times 10^{-4}$
6) $x_{1R} \times 10^{-4}$
7) $z_{1R} \times 10^{-4}$
8) $\theta_{2R} \times 10^{-3}$
9) $\theta_{3R} \times 10^{-3}$
10) Film Number

2. S4 Constants (Description)

0) 2.5×2^{-8}
1) $m_L \sin\theta_L / L_L$
2) $m_L \cos\theta_L \times 10^{-1}$
3) $m_R \sin\theta_R / L_R$
4) $m_R \cos\theta_R \times 10^{-1}$
5) $m_R \times 10^{-2}$
6) $M \times 10$
7) $z_{OL}' \times 10^{-3}$
8) $z_{OR}' \times 10^{-3}$
9) $Z_{OL}' \times 10^{-4}$
10) $Z_{OR}' \times 10^{-4}$
11) $1/nL_L$
12) $1/nL_R$
13) 1×10^{-1}
14) 1×10^{-2}
15) 1×10^{-3}
16) 0
17) $10^3/8 \times 180$
18) 5/8
19) $180 \times 10^{-3}/\pi$
20) $2^8 \times 10^{-3}$
21) 2^{-8}
22) $10^3/2^8$
23) 8×10^{-1}
24) 8×10^{-3}
25) 8×10^{-4}
26) 90×10^{-3}
27) 180×10^{-3}
28) 360×10^{-3}

C. Memory Storage

1. Preset Parameters

S3) 00F 00 400F

S4) 00F 00 20F

S5) 00F 00 70F

S6) 00F 00 91F

S7) 00F 00 100F

S8) 00F 00 140F

S9) 00F 00 200F

SK) 00F 00 280F

SS) 00F 00 306F

2. S4 Constants (Decimal Form)

0) 0.009765625

1) 0.1018

2) 0.9923

3) 0.09895

4) 0.9821

5) 0.1038

6) 0.5382

7) 0.0006204

8) 0.000646

9) 0.000655

10) 0.000673

11) 0.02369

12) 0.02404

13) 0.1

14) 0.01

15) 0.001

16) 0.0.......0

17) 0.694.....0

18) 0.625

19) 0.05729

20) 0.256

21) 0.00390625

22) 0.076525

23) 0.8

24) 0.008

25) 0.0008

26) 0.09

27) 0.18

28) 0.36

3. SS Constants (Address Changes)

0) 003F 00F

1) 00F 003F

2) 00F 006F

D. <u>S7 Cot Subroutine</u>

0)	40	23L	K5	F
1)	42	19L	L5	23L
2)	L0	28S4	32	19L
3)	50	23L	75	17S4
4)	00	3F	40	24L
5)	N0	F	50	5L
6)	26	S5	40	25L
7)	LJ	24L	50	7L
8)	26	S5	10	8F
9)	40	26L	L7	26L
10)	L2	25L	32	19L
11)	L5	26L	50	16S4
12)	66	25L	7J	23S4
13)	40	27L	50	27L
14)	7J	20S4	40	S9
15)	F5	14L	40	14L
16)	19	36F	40	28L
17)	F5	29L	40	29L
18)	L0	28L	36	20L
19)	L1	15S4	22	F
20)	L5	21L	42	14L
21)	41	29L	N0	S9
22)	26	19L	00	F
23)	00	F	00	F
24)	00	F	00	F
25)	00	F	00	F
26)	00	F	00	F
27)	00	F	00	F
28)	00	F	00	F
29)	00	F	00	F

E. <u>Heading</u>

0)	92	131F	92	259F
1)	92	2F	92	578F
2)	92	962F	92	387F
3)	92	258F	92	514F
4)	92	899F	92	387F
5)	92	322F	92	514F
6)	92	578F	92	770F
7)	92	135F	92	515F
8)	92	898F	92	514F
9)	92	962F	92	643F
10)	92	963F	92	770F
11)	92	578F	92	707F
12)	92	643F	92	131F
13)	92	3F	92	3F
14)	50	S3	50	14L
15)	26	SK	L5	10S3
16)	50	10F	50	16L
17)	26	S8	92	135F
18)	92	515F	26	500F

F. Master Program

0)	L1	S3	36	156L
1)	L5	2S3	50	1L
2)	26	S7	32	157L
3)	L5	2S3	L0	27S4
4)	36	8L	L5	S9
5)	L4	1S3	40	7S9
6)	L5	6S3	L4	25S4
7)	40	8S9	26	11L
8)	L5	1S3	L0	S9
9)	40	7S9	L5	6S3
10)	L0	25S4	40	8S9
11)	L5	8S3	50	11L
12)	26	S7	32	157L
13)	L5	8S3	L0	27S4
14)	32	16L	L5	1S9
15)	L4	7S3	40	9S9
16)	26	18L	L5	7S3
17)	L0	1S9	40	9S9
18)	L5	3S3	50	18L
19)	26	S7	32	157L
20)	L5	3S3	L0	27S4
21)	36	25L	L5	2S9
22)	L4	1S3	40	10S9
23)	L5	6S3	L4	25S4
24)	40	11S9	26	28L
25)	L5	1S3	L0	2S9
26)	40	10S9	L5	6S3
27)	L0	25S4	40	11S9
28)	L5	9S3	50	28L
29)	26	S7	32	157L
30)	L5	9S3	L0	27S4
31)	32	33L	L5	3S9
32)	L4	7S3	40	12S9
33)	26	35L	L5	7S3
34)	L0	3S9	40	12S9
35)	L5	1S3	40	4S9
36)	L5	6S3	40	5S9
37)	L5	7S3	40	6S9
38)	L5	S3	L0	4S9
39)	40	13S9	50	13S9
40)	79	6S4	L4	7S4
41)	40	14S9	50	14S9
42)	7J	1S4	L4	15S4
43)	40	15S9	50	15S9
44)	7J	14S9	40	16S9
45)	50	16S9	7J	2S4
46)	50	16S4	00	10F
47)	40	17S9	50	17S9
48)	79	22S4	L4	9S4
49)	40	18S9	L5	5S3
50)	L0	6S9	40	19S9

51)	50	19S9	7J	6S4
52)	L4	8S4	40	20S9
53)	50	20S9	7J	3S4
54)	L4	15S4	40	21S9
55)	50	21S9	7J	20S9
56)	40	22S9	50	22S9
57)	7J	4S4	50	16S4
58)	00	10F	40	23S9
59)	50	23S9	79	22S4
60)	40	24S9	L4	10S4
61)	L4	18S9	40	25S9
62)	L5	5S9	L0	4S3
63)	40	26S9	50	26S9
64)	7J	6S4	40	27S9
65)	50	27S9	7J	21S9
66)	40	28S9	50	28S9
67)	7J	5S4	50	16S4
68)	00	10F	40	29S9
69)	50	29S9	7J	22S4
70)	50	16S4	66	13S4
71)	S5	F	40	30S9
72)	L5	9S4	L0	18S9
73)	40	31S9	50	31S9
74)	7J	11S4	40	32S9
75)	50	24S9	79	12S4
76)	L4	32S9	40	33S9
77)	50	25S9	7J	15S4
78)	50	16S4	66	33S9
79)	S5	F	40	34S9
80)	7J	12S4	L4	15S4
81)	40	35S9	50	35S9
82)	7J	30S9	50	16S4
83)	00	10F	40	36S9
84)	50	36S9	7J	22S4
85)	40	38S9	50	34S9
86)	7J	13S4	40	39S9
87)	50	35S9	79	24S9
88)	50	16S4	00	10F
89)	40	37S9	50	37S9
90)	7J	22S4	L0	10S4
91)	40	40S9	L5	38L
92)	L4	1SS	40	38L
93)	L5	50L	L4	SS
94)	40	50L	L5	62L
95)	L4	SS	40	62L
96)	L5	85L	L4	SS
97)	40	85L	L5	86L
98)	L4	1SS	40	86L
99)	L5	91L	L4	SS
100)	40	91L	F5	157L
101)	40	157L	L0	1SS
102	36	103L	26	38L
103)	41	157L	L5	41S9
104)	L0	38S9	40	48S9

105)	L5	4289	L0	39S9
106)	40	49S9	L5	43S9
107)	L0	40S9	40	50S9
108)	L5	44S9	L0	38S9
109)	40	51S9	L5	45S9
110)	L0	39S9	40	52S9
111)	L5	46S9	L0	40S9
112)	40	53S9	50	48S9
113)	7J	48S9	40	54S9
114)	50	49S9	7J	49S9
115)	40	55S9	50	50S9
116)	7J	50S9	L4	55S9
117)	L4	54S9	50	117L
118)	26	S6	40	56S9
119)	50	51S9	7J	51S9
120)	40	57S9	50	52S9
121)	7J	52S9	40	58S9
122)	50	53S9	7J	53S9
123)	L4	58S9	L4	57S9
124)	NO	F	50	124L
125)	26	S6	40	59S9
126)	50	59S9	7J	56S9
127)	50	16S4	66	13S4
128)	S5	F	40	60S9
129)	50	48S9	7J	51S9
130)	40	61S9	50	49S9
131)	7J	52S9	40	62S9
132)	50	50S9	7J	53S9
133)	L4	62S9	L4	61S9
134)	50	16S4	66	60S9
135)	S5	F	40	63S9
136)	50	10F	50	136L
137)	26	S8	92	963F
138)	F5	158L	40	158L
139)	L0	2SS	32	140L
140)	26	142L	41	158L
141)	92	135F	92	515F
142	L5	143L	NO	F
143)	42	38L	NO	4S9
144)	NO	6S9	NO	F
145)	L5	144L	46	50L
146)	NO	5S9	NO	F
147)	L5	146L	46	62L
148)	NO	38S9	NO	F
149)	L5	148L	46	85L
150)	L5	151L	NO	F
151)	42	86L	NO	39S9
152)	NO	40S9	NO	F
153)	L5	152L	46	91L
154)	50	S3	50	154L
155)	26	SK	26	L
156)	0F	F	26	159L
157)	00	F	00	F
158)	00	F	00	F

159)	50	S3	50	159L
160)	26	SK	26	L
161)	24	470N		

BIBLIOGRAPHY

1. C. N. Yang and T. D. Lee, Phys, Rev. 104, 254 (1956).
2. D. Berley, T. Coffin, L. Garwin, L. M. Lederman, and M. Weinrich, Phys. Rev. 106, 835 (1957).
3. R. A. Swanson, Phys. Rev. 112, 580 (1958).
4. J. Ballam. Private Communication.
5. T. D. Lee and C. N. Yang, Phys. Rev. 105, 1671 (1957).
6. R. R. Crittenden, W. D. Walker, and J. Ballam, Phys. Rev. (to be published)
7. J. Rainwater, Ann. Rev. Nuclear Sci. 7, 1 (1957).
8. B. Rossi, High-Energy Particles (Prentice-Hall Book Company, Inc., New York, 1951) p. 43
9. C. R. Wylie Jr., Advanced Engineering Mathematics (McGraw-Hill Book Company, Inc., New York, 1951) p. 527.
10. J. Scandrett, Private Communication.
11. T. Coffin, R. L. Garwin, L. M. Lederman, S. Penman, and A. M. Sachs, Phys. Rev. 106, 1108 (1957).
12. R. E. Marshak, Meson Physics (Dover Publications, Inc., New York, 1952) p. 207
13. J. Huang, Private Communication.